Multiphysics Analysis of Millimeter-Wave Absorber with High-Power Handling Capability

Panjun Gong, *Student Member, IEEE*, Lie Liu, *Senior Member, IEEE*, Yihong Qi, *Senior Member, IEEE*, Wei Yu, *Member, IEEE*, Fuhai Li, and Ying Zhang

***Abstract*—For the fifth generation wireless communication system, millimeter-wave absorber has been frequently used in the measurement of high-power devices, such as transmitting antennas of base stations or satellite communication antennas, etc. The overheat inside the absorber can always be a matter of concern because it may lead to catastrophic fire in the anechoic chamber. A novel pyramidal structure with vent holes and heat sinks was proposed to improve the heat dissipation. The power-handling capability of the wave absorber could be improved by increasing the heat dissipation path without changing the characteristics of the base material. Multiphysics simulation was carried out to analyze the thermal-electromagnetic interaction. This absorber can be used to measure the high-power antenna and the radar system inside anechoic chambers, with power density up to 7 kW/m^2.**

***Index Terms*—Anechoic chamber, multiphysics analysis, power handling capability, radar absorbing materials.**

I. Introduction

THE anechoic chambers have been employed in the measuring of the radiation pattern of antennas and electromagnetic scattering of aircrafts for more than half century. The development of the wave-absorbing materials in certain sense made a solid foundation for the engineering of the anechoic chambers, which plays a key role in the testing of EMC/EMI, radar crossing section as well as over the air performance of various EM devices [1]. Historically, cone-shaped, or pyramidal absorbers were commonly employed in various measurement chambers to emulate the nonreflection testing environment. The high absorption of such materials must be consolidated with low reflection in the same frequency band. Hence, the dielectric permittivity and magnetic permeability of the materials need to be properly customized to achieve the best impedance matching, as well as maximum attenuation over broad frequency band.

Thermoset or thermoplastic polymer foam in anechoic chamber is low density and porous structure containing conductive filler. Conventionally, they are dielectric absorbers with frequency-dependent dielectric permittivity, which exhibit high losses owing to the relaxation dispersion of the conductive additions, such as carbon black, carbon fiber, multiwall carbon nanotubes, or carbonyl iron fiber, etc. [2]. Traditionally, polyurethane (PU) foam has been employed in an anechoic chamber since 1960s, owing to their good absorption properties, simple process technology as well as low cost [3], [4]. However, with the ever-increasing demand of cleanness and life span, PU-based soft foam faces great challenges. Recently, hard foam absorbing materials have begun to use in EMC/EMI chambers. This novel absorber is mostly made of polyolefin resin, such as polyethylene, polypropylene, and polystyrene, together with conductive powder. Injection molding process instead of wire cutting was employed in the process of hard form, with features like high-dimension accuracy, clean and environment-friendly, long life and many other advantages. Among these hard foams, expanded polypropylene (EPP) has the outstanding mechanical properties [5], [6]. Many conductive fillers can be mixed with EPP resin. However, considering the mature mixing process of mass production, conductive carbon black is commonly used as the filler. Due to the close-cell microstructure and low thermal conductivity, EPP hardly withstands high-power radiation from airborne radar or satellite radar under test [4].

For the fifth generation wireless communication system (5G), the power density of the base station could be much higher than that in 4G. The main reason lies on the narrower beam width and higher radiation power to overcome the high path loss as compared to that in 4G. For the measurement inside anechoic chamber, if the beam width is too narrow or the power level is too high, the radiation EM energy may cause overheat of the absorber under radiation, or even burn of the whole chamber. The traditional solution is to use hollow pyramid to replace the solid one to facilitate heat transfer. However, the absorption property of the hollow absorber can be inferior, as compared to the solid absorber with the same height.

Nonflammable wedge absorber using hard PU foam with heat-resistant temperature up to 120 °C was developed [7]. However, the reflectivity is about −25 dB for frequency above 1 GHz when the total height is 60 cm. Hence, it is not suitable for high-performance anechoic chamber with the reflectivity

Manuscript received April 30, 2017; revised June 7, 2017; accepted June 7, 2017. Date of publication June 23, 2017; date of current version August 17, 2017. This work was supported by the National Science Foundation of China under Grant 61671203, and Ministry of Education–China Mobile Research Foundation (No. MCM 20150101). The associate editor coordinating the review of this manuscript and approving it for publication was J. Fan. *(Corresponding Author: Lie Liu.)*

P. Gong and F. Li are with the College of Electrical and Information Engineering, Hunan University, Changsha 410006, China, (e-mail: panjun.gong@generaltest.com; fuhai-li@vip.sina.com).

L. Liu, Y. Qi, and W. Yu are with the College of Electrical and Information Engineering, Hunan University, Changsha 410006, China, and also with General Test Systems Inc., Shenzhen 518102, China (e-mail: liulie_leo@hotmail.com; yihong.qi@generaltest.com; fred.yu@generaltest.com).

Y. Zhang is with the General Test Systems Inc., Shenzhen 518102, China (e-mail: ying.zhang@generaltest.com).

Color versions of one or more of the figures in this paper are available online at http://ieeexplore.ieee.org.

Digital Object Identifier 10.1109/TEMC.2017.2714900

below −50 dB at 10 GHz or above. Hollow pyramid absorber developed by the same company could have much higher power handling capability, for example, up to 20 kW/m^2. However, neither the low- nor the high-frequency performance could meet the requirement of the normal microwave chamber [7].

Aramid Honeycomb coated with a layer of high loss conductive absorber was developed for extreme high-power applications [8]. The power handling capability can be up to 15.5 kW/m^2 and the maximum working temperature can be up to 140 °C. However, the cost of the aramid honeycomb-based high-power materials can be much more expensive than absorber made of polymeric foam. It is not a cost-effective solution for the large chamber, but a solution for certain location inside chamber, like the wall facing to the antenna under test.

In this paper, we propose a kind of EPP pyramid absorber with vent holes and heat sinks to improve the circulation of the thermal energy generated internally. Also, a metal fin is embedded inside the foam pyramid to dissipate heat by conduction instead of convection, which is more effective. Multiphysics analysis of the thermal-electromagnetic interaction validates the feasibility of the design. The theory and design methodology is elaborated in Sections II and III before the discussion of simulation results and conclusions.

II. Multiphysics Modeling

A. Electromagnetic Modeling

ANSYS Electronics Desktop, which bases on the finite element method and the time-domain solver of Maxwell's Equations to generate an electromagnetic field solution, was employed in this study. In general, the finite element method divides the full problem space into thousands of smaller regions and represents the field in each subregion with a local function [9].

To generate a solution from where S-parameters can be computed, HFSS employs the mixed-potential integral equation method. Once the 3-D surfaces mesh generated, the following equation is applied to it [9]:

$$\hat{n} \times (-j\omega\vec{A} - \nabla\phi) = \hat{n} \times Z_S \vec{J} \tag{1}$$

where $\hat{n}$ is a unit vector perpendicular to the face of the triangles, j is the imaginary unit, ω is the angular frequency, $\vec{A}$ is the magnetic vector potential, ϕ is the electric potential, Z_S is the surface impedance, and $\vec{J}$ is the current density.

According to the classical EM field theory, it is desirable that incident EM waves on the surface of the material may penetrate the material as much as possible. The absorbers have efficient absorption of incident EM waves by converting EM energy into heat. The reflectivity of a planar absorbing material can be expressed as follows [10]:

$$\Gamma = 20 \lg \left| \frac{Z - Z_0}{Z + Z_0} \right| \tag{2}$$

where $Z_0 = \sqrt{\mu_0/\varepsilon_0}$ is the characteristic impedance of vacuum, and $Z = \sqrt{\mu/\varepsilon}$ is the characteristic impedance of the material.

The absorption of the absorber includes both the conduction loss and the dielectric loss. It mainly comes from electron polarization, atomic polarization, intrinsic electric dipole orientation polarization and interfacial polarization, and so on. P_d, the power dissipated per unit volume at the center of the unit cell is calculated by

$$P_d = (\omega\varepsilon_0\varepsilon'' + \sigma)\left|\vec{E}\right|^2 \tag{3}$$

where $|\vec{E}|$ is the magnitude of electric field, ε_0 is the permittivity of free space, ε'' is the imaginary part of the complex permittivity, and σ is the conductivity of the material.

According to the law of conservation of energy, it can be considered that the EM energy attenuated inside material is fully converted into thermal energy.

B. Modeling of Heat Transfer

ANSYS mechanical was employed to analyze the temperature distributions inside the absorber. The principle for thermal analysis in ANSYS is a heat balance equation obtained from the principle of conservation of energy. The finite element simulation was run with Mechanical solver to calculate nodal temperatures, then the nodal temperature was used to obtain other thermal quantities [11].

The heat generation term in a specific unit cell can be given by the specific dissipation times the volume of the cell as shown in

$$Q = P_d \delta x \delta y \delta z. \tag{4}$$

The heat transfer phenomena consist of conduction, convection, and heat radiation. In most cases, three types of heat transfer occur at the same time, called the compound heat transfer process.

In this study, only heat conduction and convection were taken into account due to the relative low-limit temperature of hard foam, in which heat radiation is negligible.

On the surfaces of material, convective boundary conditions for heat transfer is applied to the following Newton's law of cooling:

$$q^n = hA(T_S - T_B) \tag{5}$$

where q^n is the heat transfer rate, h is the convection heat transfer coefficient, A is the surface area, T_S is the surface temperature of the material, and T_B is the temperature of the surrounding air.

The governing equation of heat conduction is expressed by [12]

$$\rho_m c_m \frac{\partial T}{\partial t} = -div\vec{q} + Q \tag{6}$$

where T is the temperature inside material, ρ_m is the density of a material, c_m is the specific heat capacity, $\vec{q}$ is the heat flow rate vector per unit volume, and Q is the heat generation term per unit volume due to the incident EM wave.

In Cartesian coordinates, Fourier's conduction law for an anisotropic body is

$$\vec{q} = -\vec{k}\nabla T \tag{7}$$

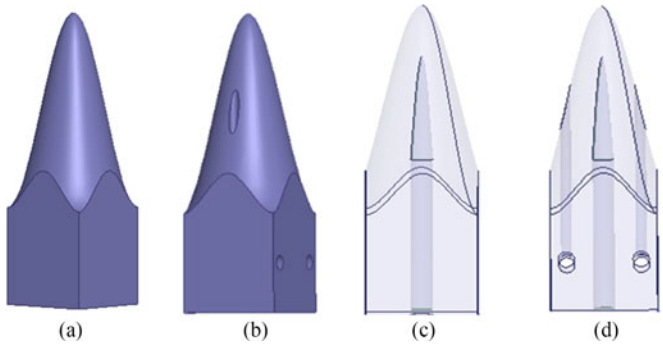

Fig. 1. EPP absorber: (a) the original pyramid, (b) with vent holes, (c) with heat sinks, (d) with both vent holes and heat sinks.

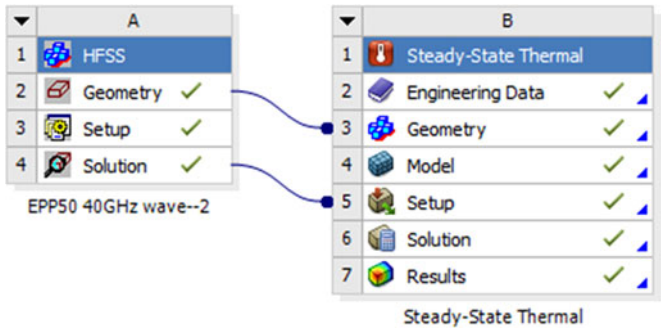

Fig. 2. Links between HFSS and stead-state thermal.

where

$$\vec{k}(T,\alpha) = \begin{bmatrix} \vec{k}_{xx} & \vec{k}_{xy} & \vec{k}_{xz} \\ \vec{k}_{yx} & \vec{k}_{yy} & \vec{k}_{yz} \\ \vec{k}_{zx} & \vec{k}_{zy} & \vec{k}_{zz} \end{bmatrix}$$

$$\nabla T = \begin{Bmatrix} \frac{\partial T}{\partial x} \\ \frac{\partial T}{\partial y} \\ \frac{\partial T}{\partial z} \end{Bmatrix}.$$

In (7), ∇ denotes the gradient operator and $\vec{k}$ is the anisotropic thermal conductivity matrix.

III. Numerical Simulation

Multiphysics simulation was carried out to calculate the electromagnetic and thermal coupling with a commercial finite element software, ANSYS 17.2. It offers a comprehensive solution of coupled analysis between EM and thermal. In this study, the analysis of the thermal-electromagnetic interaction is a closed-feedback process. The temperature distribution inside absorber was calculated when the absorber is under the radiation of vertical incident plane waves.

A. Full-Wave Electromagnetic Simulation

The absorber is heated up under electromagnetic radiation due to the presence of inherent material losses. In this study, no magnetic losses were taken into consideration because both EPP and carbon are nonmagnetic materials. The surface loss density and the volume loss density of the pyramid absorber are simulated except for reflectivity calculation.

EPP absorber can be considered as a periodic structure composed of many pyramids. Only a unit pyramid applied with periodic boundary conditions needs to be calculated. The absorbers analysis model is set up as shown in Fig. 1. The overheating inside the absorber under high-power field will result in the rapid change of the wave absorption characteristics of the absorber. To solve the matter, without deteriorating the reflectivity of the absorber, the first solution is that vertical vent holes were drilled on the top of the pyramidal absorber as shown in Fig. 1(b). Alternative solution is that a low-scattering bar connected to the metal plate is embedded in the interior of the pyramid absorber as shown in Fig. 1(c). A pyramid absorber equipped with both vent holes and heat sinks is shown in Fig. 1(d).

B. Thermal Simulation

Thermal analysis calculates the temperature distribution and related thermal quantities of the pyramid absorber, which includes both steady-state thermal and transient thermal analysis.

First, the HFSS project contains the electromagnetic calculation results, in which dielectric loss power density needs to be imported into ANSYS Workbench (WB). The second step is to add the steady-state thermal solution to WB. The third step is to link the HFSS project with thermal solution in WB as shown in Fig. 2. The fourth step is to set up thermal property in the input data of thermal solution. The corresponding thermal materials are selected in the database of the software. The isotropic thermal conductivity of the absorbing material was set to 0.042 W/m·°C. The fifth step is to update the project and assign materials for all geometries of the model. The sixth step is to apply heat generation load for the absorber model and the heat flux load for the outer faces, also it is needed to assign the convective boundary condition on the surfaces of the absorber. Due to the relative low surface temperature, the contribution from heat radiation is negligible. Finally, thermal analysis and temperature distribution results of the absorber are calculated.

According to the temperature distribution results of thermal simulation, the size and direction of vent holes and the shape and size of low-scattering bar are optimized to reduce the internal temperature of the pyramid absorber.

IV. Results and Discussion

A. Temperature Distribution of EPP Absorber Under High Radiation Power

When the temperature is below 110 °C, the performance and physical property of the EPP absorber will be not deteriorated, so this temperature can be used to estimate the power limit that the absorber can handle. Convection mechanism can be divided into two categories: natural and forced convection. Natural convection coefficient varies from 1 to 25 W/m^2 °C [10]. The power density of the incident plane waves was 3 kW/m^2, and the natural convection coefficient was set to 5 W/m^2 °C. The calculated temperature distribution of EPP pyramid absorber under high-power radiation tests is shown in Fig. 3.

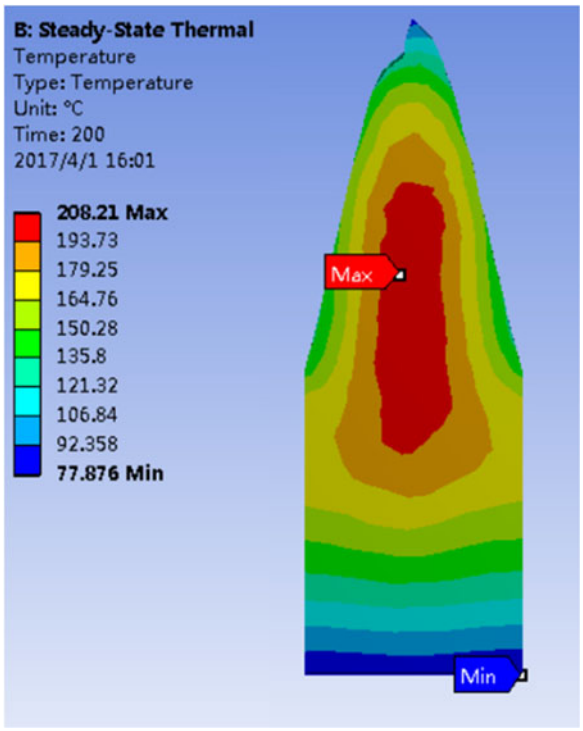

Fig. 3. Temperature distribution inside absorber under high-power incident wave in air.

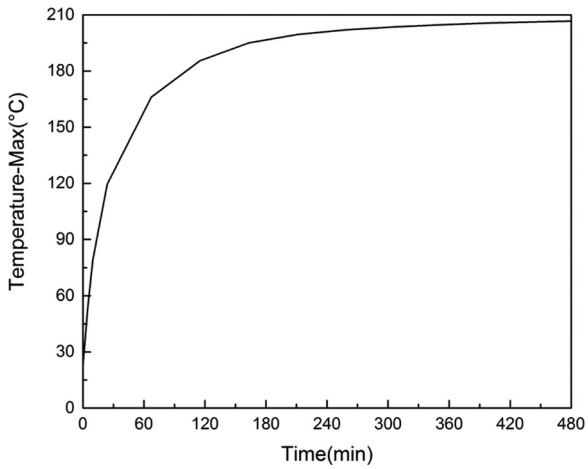

Fig. 4. Maximum temperature of the absorber with irradiation time in air.

The maximum temperature inside absorber is above the limit that the absorber cannot withstand this radiation power under normal working conditions.

It is shown in Fig. 3 that under a high-power radiation source, the temperature of the center of the pyramidal absorber is the highest and the temperature of the base portion bonded to the metal plate is the lowest, because the surface temperature of the pyramid wave absorber can be reduced by the convection of the air, and the heat of the base can be conducted through the metal plate. Fig. 4 shows the relationship of the maximum internal temperature versus time. It can be seen that more than 3 h is needed to reach the equilibrium temperature. It means that time is a quite important factor for the measurement of high-power antenna, which should be carefully controlled to avoid overheat of the chamber's absorber.

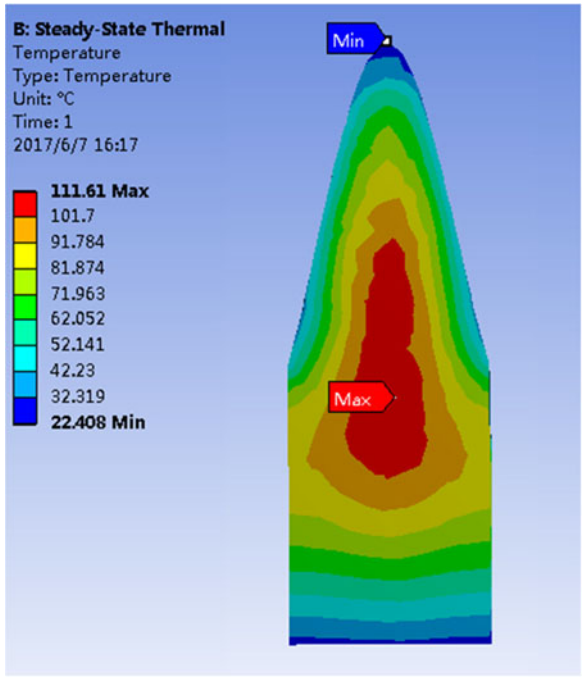

Fig. 5. Temperature distribution inside absorber under high-power incident wave by forced air cooling.

In order to reduce the temperature inside the absorber, an effective means is forced cooling. The forced air convection coefficient was set to 30 W/m^2 °C. The temperature distribution inside the absorber is shown in Fig. 5. It can be found that the internal temperature of the absorber is significantly reduced.

B. Temperature Distribution of EPP Absorber With Vent Holes

In order to further reduce the internal temperature, without changing the thermal property of the material, vertical vent holes were drilled on the top of the pyramidal absorber and longitudinal or transverse holes were made inside the base of the absorber. The temperature of the absorber is reduced by forced air cooling. The vertical holes were connected to the longitudinal and transverse holes, and the longitudinal and transverse holes of the base of the absorbers were also connected, so that the air in the anechoic chambers can be discharged to outside. The diameter of the vertical holes is preferably less than $\lambda/2$ to avoid the resonance and reflection due to the size of the venting hole.

The power flux density of the plane wave on the surface of the material was set to 3 kW/m^2, and the forced air convection coefficient was set to 30 W/m^2 °C. The temperature distribution inside the absorber with vertical and transverse holes is shown in Fig. 6. The internal temperature of the absorber is decreased to a certain degree as compared to the maximum temperature in Fig. 5.

When the different types of vent holes are drilled on the pyramid absorber, their reflection coefficient curves are shown in Fig. 7. The black solid shows the reflectivity of original absorbers. The red dash shows the reflectivity of the absorbers

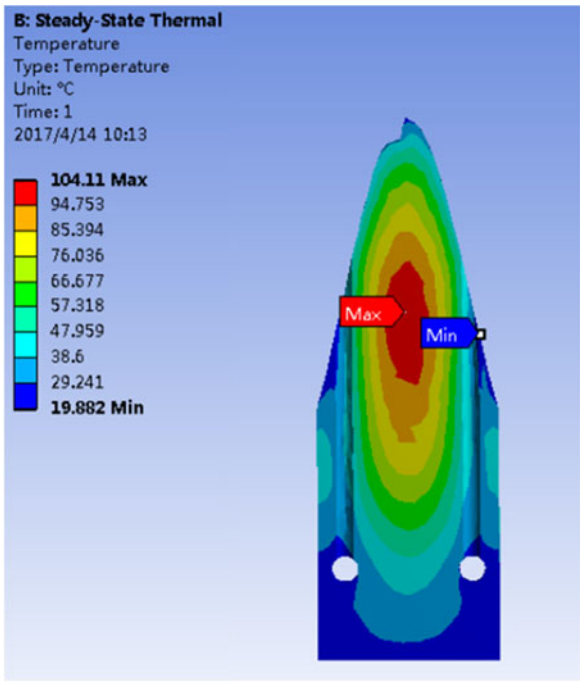

Fig. 6. Temperature distribution inside the absorber with vent holes.

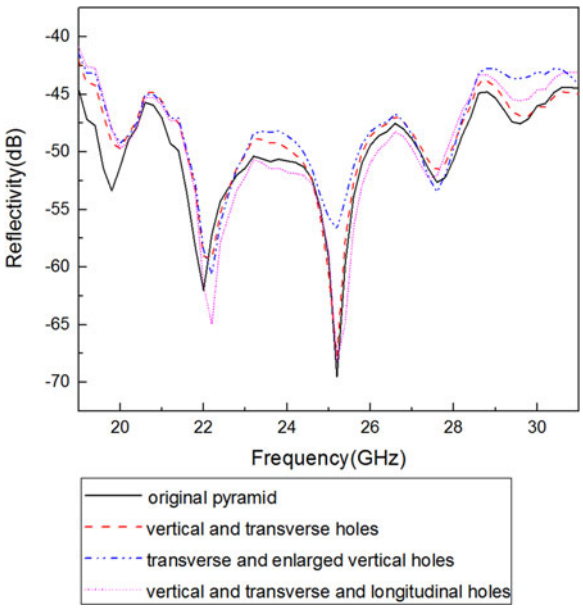

Fig. 7. Reflection coefficient curves of absorbers with different types of vent holes.

with vertical and transverse holes whose maximum temperature is 104.1 °C. The blue dash dot dot line shows the reflectivity of the absorbers with transverse and enlarged vertical holes, whose maximum temperature is 103.9 °C. The pink short dot is the reflectivity of the absorbers with vertical and transverse and longitudinal holes whose maximum temperatures are 103.1 °C. It can be concluded from Fig. 7 that enlarging the vertical cooling holes affects the reflectivity of the absorber, but cannot obviously improve the heat dissipation. So, it is not advisable to improve the heat dissipation by increasing the aperture.

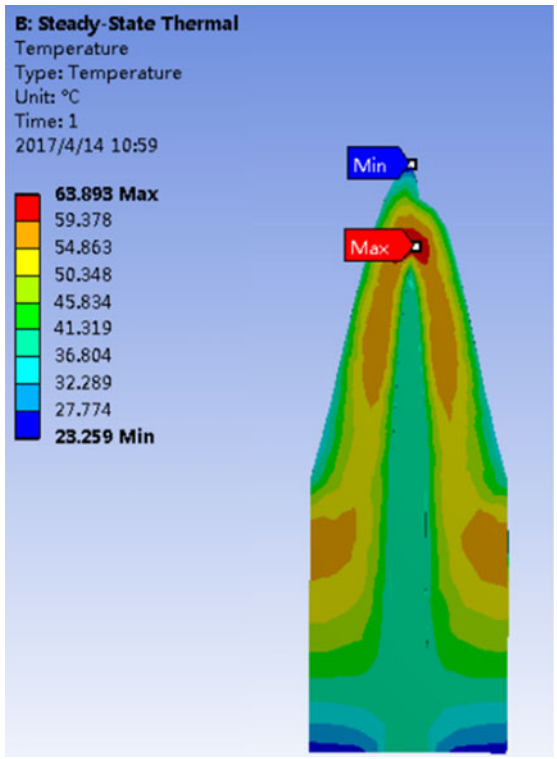

Fig. 8. Temperature distribution inside the absorber with heat sinks.

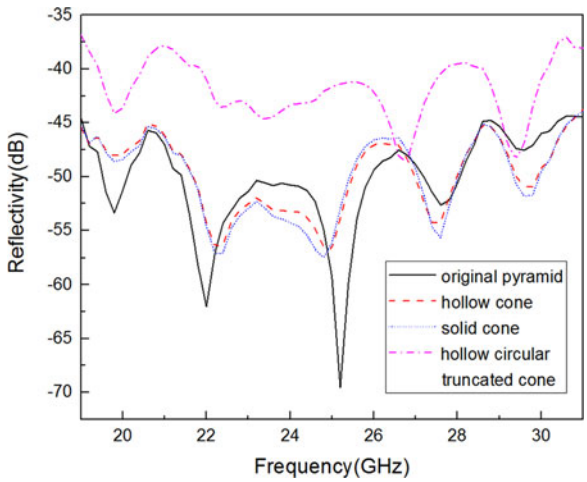

Fig. 9. Reflection coefficient curves of absorbers with different types of heat sinks.

C. Temperature Distribution of EPP Absorber With Heat Sinks

In order to further reduce the internal temperature of the absorber, a low-scattering metal bar connected to the metal plate was embedded in the interior of the pyramid absorber. The heat at the center of the pyramidal absorber was dissipated by conduction, and the heat is dissipated into the air through the metal plate.

The power flux density of the surface of the material remains constant and the natural convection coefficient was set to 5 $W/m^2 \cdot °C$. The temperature distribution inside the absorber under the same condition is shown in Fig. 8. The internal temperature of the absorber with heat sinks was significantly decreased.

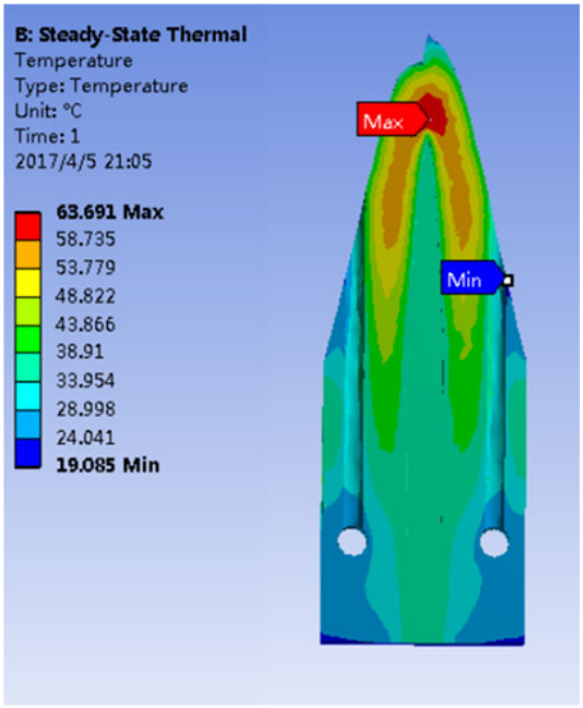

Fig. 10. Temperature distribution inside the absorber with vent holes and heat sinks.

Compared with heat transfer by air convection of the vent holes, thermal conductance of heat sinks is more effective.

As long as the reflectivity of the absorber is not significantly deteriorated, the heat sinks can have various shapes. When the heat sinks with different shapes are embedded in the interior of pyramid absorber, their reflection coefficient curves are shown in Fig. 9. Considering the convenience of installation and the reflection of millimeter waves, the cone-shaped heat sink can be chosen. If the weight of the absorber is taken into consideration, the hollow-type heat sink is more preferred.

Under the same incident power density, the maximum steady-state temperature of the absorbers with hollow-type pointed cone, solid-type pointed cone, and hollow-type circular truncated cone are 63.9 °C, 63.6 °C, and 65.2 °C, respectively.

D. Temperature Distribution of EPP Absorber With Both Vent Holes and Heat Sinks

A pyramid absorber equipped with both vent holes and heat sink was also developed. The power flux density of the surface of the material remains constant and the forced air convection coefficient was set to 30 W/m$^2\cdot$°C. The structure and temperature distribution inside the absorber are shown in Fig. 10. The comparison of the reflectivity of four different structures is shown in Fig. 11. The maximum power density that original millimeter-wave EPP pyramid absorber can handle is 1 kW/m^2. The EPP pyramid absorber with vent holes and heat sinks can handle the maximum power density up to 7 kW/m^2 and the internal temperature is still within the limit of EPP materials. The reflectivity of original absorbers and redesigned absorbers under oblique incidence are compared in Table I. It can be concluded that the embedded heat sink bar does not deteriorate the reflectivity of oblique incidence significantly.

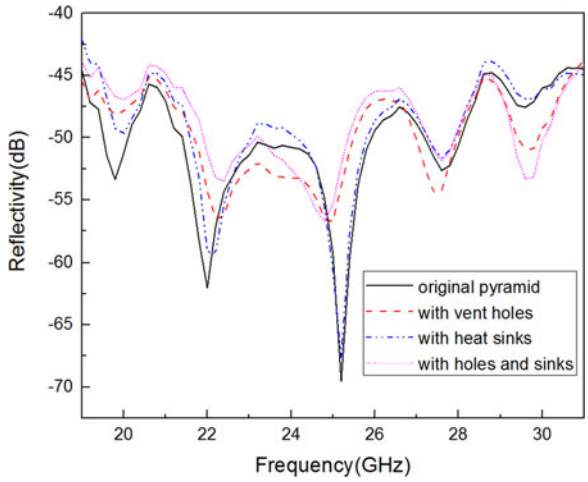

Fig. 11. Reflection coefficient of absorbers with different structures of heat dissipation.

TABLE I
REFLECTIVITY OF THE ORIGINAL AND THE REDESIGNED ABSORBER WITH HIGH POWER HANDLING CAPABILITY

Absorber types / Incident angel	The reflectivity	
	The original absorber(dB)	The redesigned absorber(dB)
0°	-44	-44
15°	-40	-43
30°	-43	-38
45°	-42	-40

According to the simulation results, it can be concluded that this novel structure with heat sink and vent holes has better heat dissipation and higher power handling capacity.

V. CONCLUSION

EPP pyramid absorber with high-power handling capability was investigated by numerical simulation. Without changing the thermal property of the base materials, vent holes and heat sinks which can improve heat dispassion were integrated into the EPP absorber in line with the optimized reflectivity. The proposed high-power EM absorber can have power handling capability up to 7 kW/m^2, which is a promising candidate for the measurement of radar or phase array antenna in millimeter frequency with high-radiation power.

REFERENCES

[1] P. Shen, Y. Qi, W. Yu, F. Li, and J. Fan, "Fast method for OTA performance testing of transmit-receive cofrequency mobile terminal," *IEEE Trans. Electromagn. Compat.*, vol. 58, no. 4, pp. 1367–1374, Aug. 2016.

[2] L. B. Kong *et al.*, "Recent progress in some composite materials and structures for specific electromagnetic applications," *Int. Mater. Rev.*, vol. 58, no. 4, pp. 203–259, 2013.

[3] W. H. Emerson, "Electromagnetic wave absorbers and anechoic chambers through the years," *IEEE Trans. Antennas Propag.*, vol. AP-21, no. 4, pp. 484–490, Jul. 1973.

[4] L. H. Hemming, *Electromagnetic Anechoic Chambers: A Fundamental Design and Specification Guide.* Hoboken, NJ, USA: Wiley, 2002.

[5] W. Zhai, Y.-W. Kim, and C. B. Park, "Steam-chest molding of expanded polypropylene foams. 1. DSC simulation of bead foam processing [J]," *Ind. Eng. Chemistry Res.*, vol. 49, no. 20, pp. 9822–9829, 2010.
[6] W. Zhai, Y.-W. Kim, D. W. Jung, and C. B. Park, "Steam-chest molding of expanded polypropylene foams. 2. Mechanism of interbead bonding [J]," *Ind. Eng. Chemistry Res.*, vol. 50, no. 9, pp. 5523–5531, 2011.
[7] Radio Wave Absorber, Vol. 2, Token EMC Engineering Co. Ltd., 2011. [Online] Available: http://www.tee.tokin.jp/eng/index.html
[8] High Power Broadbanded Pyramidal Honeycomb RF Absorber, Technical Bulletin 390-16, Cuming Microwave, 2012. [Online]. Available: https://www.cumingmicrowave.com
[9] HFSS Online Help, Release 17.2, ANSYS, Inc, 2016. [Online]. Available: http://www.ansys.com/
[10] E. F. Knott, J. F. Shaeffer, and M. T. Tuley, *Radar Cross Section*, 2nd ed. Norwood, MA, USA: Artech House, 1993.
[11] ANSYS Mechanical APDL Thermal Analysis Guide, Release 15.0, ANSYS, Inc, 2013. [Online]. Available: http://www.ansys.com/.
[12] J. P. Holman, *Heat Transfer*, 10th ed. Boston, MA, USA: McGraw-Hill, 2010.

Panjun Gong (S'16) received the B.Sc. degree in electronic information engineering from the University of South China, Hengyang, China, in 2011, and he is currently working toward the M.Sc. degree in electronics from the Hunan University, Changsha, China.

His research interests include microwave technique and antenna design.

Lie Liu (M'09–SM'12) received the B.Sc. degree in material science and engineering from the Beijing University of Aeronautics and Astronautics, Beijing, China, in 1991, and the M.Sc. degree in material science from the China Academy of Launch-Vehicle Technology, Beijing, in 1994, and the Ph.D. degree in mechanical engineering from Nanyang Technological University, Singapore, in 2003.

From 2002 to 2012, he had been a Senior Research Scientist in Advanced Materials Group of Temasek Laboratories, National University of Singapore. From 2012 to 2015, he had been a Technical Director of Kuang-Chi Institute of Advanced Technologies, Shenzhen, China. Since 2015, he has been a chief technical officer of General Test Systems, Shenzhen, China, and adjunct professor of Hunan University, China. He has published more than 50 papers in journals and conferences, and one book chapter. His research interests include EM materials, measurement of wireless communication systems, and anechoic chamber.

Yihong Qi (M'92–SM'11) received the B.S. degree in electronics from the National University of Defense Technologies, Changsha, China, in 1982, and the M.S. degree in electronics from the Chinese Academy of Space Technology, Beijing, China, in 1985, and the Ph.D. degree in electronics from Xidian University, Xi'an, China, in 1989.

From 1989 to 1993, he was a Postdoctoral Fellow and then an Associate Professor with the Southeast University, Nanjing, China. From 1993 to 1995, he was a Postdoctoral Researcher at McMaster University, Hamilton, ON, Canada. From 1995 to 2010, he was with Research in Motion (Blackberry), Waterloo, ON, where he was the Director of Advanced Electromagnetic Research. He is currently the President and Chief Scientist with General Test Systems, Inc., Shenzhen, China; he founded DBJay in 2011, and he is the CTO of ENICE. He is also an Adjunct Professor in the EMC Laboratory, Missouri University of Science and Technology, Rolla, MO, USA, and an Adjunct Professor in Hunan University, Changsha. He is an inventor of more than 200 published and pending patents.

Dr. Qi was a Distinguished Lecturer of IEEE EMC Society for 2014 and 2015, and serves as the Chairman of the IEEE EMC TC-12.

Wei Yu (M'13) received the B.S. degree in electrical engineering from Xi'an Jiaotong University, Xi'an, China, in 1991, the M.S. degree in electrical engineering from the China Academy of Space Technology, Beijing, China, in 1994, and the Ph.D. degree in electrical engineering from Xidian University, Xi'an, in 2000.

From 2001 to 2003, he was a Postdoctoral Fellow with the University of Waterloo, Waterloo, ON, Canada. He was a CTO with Sunway Communications Ltd., from 2008 to 2012. He founded Antennovation Electronics Inc. in 2004 and cofounded General Test Systems Inc., Shenzhen, China, in 2012. He is currently with DBJ Technologies as COO. His current research interests include signal processing and mobile device test system. He is an inventor of 32 published and pending patents.

Fuhai Li received the B.S. and M.S. degrees in instrument science and technology from Hunan University, Changsha, China, from 1982 to 1988.

He is currently a Professor at Hunan University, Changsha. During his tenure, he had received several science and technology progress awards. He has published more than 20 papers in the national core journals.

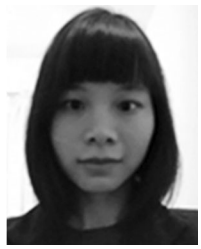

Ying Zhang received the Master's degree in materials science and engineering from Hubei University, Wuhan, China, in 2014.

She is currently a Material Engineer in Shenzhen General Test System Inc. (GTS), and is in the charge of the development of microwave absorbing materials. She has published several research papers on rubber pyramid absorbing materials and series of expandable polypropylene absorbing materials during her work in GTS.